

Sign-alternating current structure and oscillations in I – V characteristics of a metal plate

N M Makarov†, G B Tkachev†, V A Yampol'skii†, L M Fisher‡ and I F Voloshin‡

† Institute for Radiophysics and Electronics, Ukrainian Academy of Science, Akademika Proskura Street 12, Kharkov, 310085, Ukraine

‡ All-Russian Electrical Engineering Institute, Krasnokazarmennaya Street 12, Moscow, 111250, Russia

Received 12 September 1994

Abstract. We study the features of the current density distribution in a thin plate of a compensated metal under pinch-effect conditions. It is established that the current structure possesses a sign-alternating character. There exist space layers where the current flows in the opposite direction to an electric field in the sample. The current density spatial oscillations are caused by the non-linearity stipulated by the influence of a non-uniform magnetic field of the current on the metal conductivity. It is shown that the sign-alternating current distribution results in oscillations in the sample I – V characteristics. These oscillations are observed experimentally.

1. Introduction

An electric current flowing in a metal is the source of a magnetic field which affects the dynamics of conducting electrons. This influence results in a dependence of the sample conductivity on the distribution of the intrinsic magnetic field of the current. This magnetodynamic mechanism of non-linearity is typical for pure metals at low temperatures. In a static case, the magnetodynamic non-linearity is highly pronounced under conditions of the classical size effect, where it causes a deviation in the I – V characteristics (CVC) of the sample from Ohm's law. In this paper we shall analyse the non-linear conductivity of a metal plate whose thickness d is much less than the electron mean free path l :

$$d \ll l. \quad (1.1)$$

We shall assume that electron scattering on a sample surface is diffuse.

Such an analysis for the case of relatively weak currents was first carried out in [1, 2]. It was noted therein that a group of trapped electrons is formed inside the plate as a result of the influence of the intrinsic magnetic field of the current on the electron motion. The trapped electrons appear in the sample owing to the antisymmetry of the magnetic field distribution. They wind around a plane where the magnetic field changes sign, do not collide with the diffuse plate boundaries, and interact with the electric field over their entire free path. For small enough values of the current to ensure that the inequality

$$d < R \quad (1.2)$$

holds, the relative number of the trapped electrons is of the order of $(d/R)^{1/2}$. Here $R \sim cp_F/eH$ is the characteristic radius of curvature of the electron trajectory in the intrinsic magnetic field of the current, H is the value of this field at the sample surface:

$$H = \frac{2\pi I}{c} \quad (1.3)$$

I is the current per sample width, $-e$ and p_F are the charge and the Fermi momentum of an electron, and c is the speed of light. The trapped electron conductivity may be evaluated as

$$\sigma_{\text{trap}} \simeq \sigma_0 \left(\frac{d}{R} \right)^{1/2} \propto I^{1/2}. \quad (1.4)$$

It increases as the current increases, and becomes dominant within the interval of the currents where

$$d \ll (Rd)^{1/2} \ll l. \quad (1.5)$$

Here σ_0 is the static conductivity of a bulk sample and $(Rd)^{1/2}$ is the characteristic length of a trapped electron trajectory arc. For this reason the linear portion of the CVC, which holds in the interval

$$d \ll l \ll (Rd)^{1/2} \quad (1.6)$$

is replaced by a square-root form under conditions (1.5).

It should be noted that, in contrast to other known non-linear mechanisms, the magnetodynamic non-linearity results in a decrease in sample resistance in the weak-current region (1.2). This effect has been observed in Zn [3] and Ga [4], and was investigated in detail for W and Cd [5, 6].

The analysis of the magnetodynamic non-linearity in the range of strong currents, where the condition

$$R \ll d \quad (1.7)$$

is satisfied, shows [7] that a strong pinch-effect takes place in plates of compensated metals. The current density proves to be highest within a layer about $8R$ in thickness near the middle of the sample. The conductivity in this pinch layer is determined by the trapped electrons (trajectory I in figure 1) and is of the order of σ_0 . Outside this central region the electrons move in the strong magnetic field of the current along a near-circular Larmor orbit, whose radius is about R . Therefore, their contribution to the conductivity is much smaller than σ_0 . If one neglects this contribution, the voltage will increase quadratically with current in the region (1.7).

Thus, the magnetodynamic non-linearity results in an increase of the plate resistance in strong currents. This statement is in accordance with the experimental data [4–6]. It should be noted that the increase of the resistance was accompanied by the CVC oscillations. The nature of these oscillations has not yet been understood. The main aim of this paper is to propose a possible explanation of the origin of this phenomenon.

We associate these oscillations with the contribution of the Larmor electrons to the metal conductivity under conditions of the pinch effect mentioned above. According to

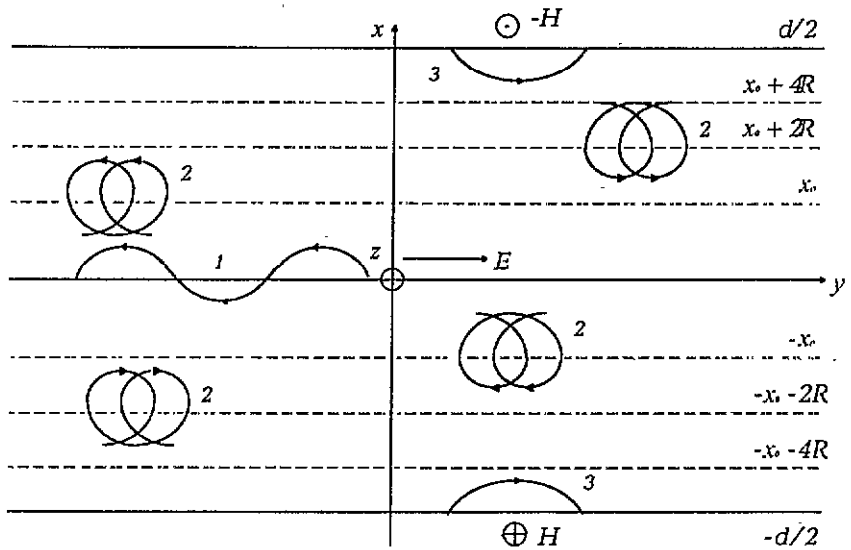


Figure 1. Schematic representation of the geometry of the problem and trajectories of the trapped (1), Larmor (2), and surface (3) electrons in the intrinsic magnetic field of the current.

our analysis, the conductivity of this group is caused by the drift of the electron orbits in the non-uniform intrinsic magnetic field of the current. Therefore, there exists a non-local relationship between the current density of the Larmor electrons and the gradient of the magnetic field. This relationship provides a trajectory transfer of the current from the pinch layer to the periphery of the sample. As a result, the sign-alternating current structure appears. This means that the peripheral part of the plate turns out to be broken into Larmor-current layers with a thickness of about $2R$. The sign of the current density differs in the neighbouring layers. The number of the current layers depends on the value of the total current, and proves to be about $d/2R$. The increase of this number with the current is the reason for the CVC oscillations.

2. Statement of the problem: electron dynamics and current density

2.1. Geometry of the problem, magnetostatic equation and boundary conditions

We shall consider an unbounded plate of compensated metal through which a current I is flowing. The y axis is directed along the current, the x axis is normal to the plate, and the z axis is collinear to the intrinsic magnetic field $H(x)$ of the current. The origin of the coordinate system is chosen to be in the middle of the plate. We suppose that the plate thickness d is much smaller than the electron mean free path l .

We shall analyse the current density distribution assuming that the metal is isotropic. For simplicity, we shall consider the electron and hole Fermi surfaces to be identical spheres. We also assume the masses, as well as the mean free paths, of the electrons and holes to be equal. In this situation there is no Hall effect in the metal, i.e. the non-diagonal components of the conductivity tensor are equal to zero.

For the chosen geometry the magnetostatic equation has the form

$$\frac{dH(x)}{dx} = -\frac{4\pi}{c} j(x) \tag{2.1}$$

where $j(x)$ is the current density. The boundary conditions to use with this equation are

$$H(-d/2) = -H(d/2) = H. \quad (2.2)$$

From Maxwell's equation $\text{rot} \mathbf{E} = 0$ it follows that the electric field $E_y \equiv E$ within the plate is uniform.

2.2. Trapped, Larmor and surface electrons

We now discuss the dynamics of charge carriers in a strong non-uniform magnetic field $H(x)$. Since the electron and hole motion differ only in their direction, we need only consider the dynamics of the electrons. It should be kept in mind that the contributions of electrons and holes to the diagonal components of the conductivity add together, while those to the non-diagonal components compensate each other.

Let us pick a gauge for the vector potential of the form

$$\mathbf{A} = (0; A(x); 0) \quad A(x) = \int_0^x dx' H(x'). \quad (2.3)$$

The constants of electron motion in the field $H(x)$ are the total energy, which is equal to the Fermi energy

$$\varepsilon_F = p_F^2/2m \quad (2.4)$$

as well as the generalized momenta

$$p_z = mv_z \quad p_y = mv_y - eA(x)/c. \quad (2.5)$$

Here m is the electron mass, and v_z and v_y are the components of the electron velocity. The velocity component v_x is

$$v_x = \pm(1/m)[p_\perp^2 - (p_y + eA(x)/c)^2]^{1/2} \quad p_\perp = (p_F^2 - p_z^2)^{1/2}. \quad (2.6)$$

From the condition of the non-negativity of the subradical expression in (2.6), one can find the range of admissible values for the integrals of electron motion:

$$p_y^-(x) \equiv -p_\perp - eA(x)/c \leq p_y \leq p_\perp - eA(x)/c \equiv p_y^+(x). \quad (2.7)$$

This range is presented schematically in figure 2. From this figure it is clear that the electrons can be divided into three groups according to the character of their motion.

2.2.1. Trapped electrons. These electrons move along trajectories of type I in figure 1. The half period of their motion along the x axis is

$$T = \int_{x_1}^{x_2} \frac{dx'}{|v_x(x')|}. \quad (2.8)$$

The turn points $x_1 < x_2$ are the roots of the equation

$$p_y^-(x) = p_y. \quad (2.9)$$

The trapped electrons occupy the following range in momentum space (p_\perp, p_y)

$$-eA(x)/2c \leq p_\perp \leq p_F \quad p_y^-(x) \leq p_y \leq p_y^+(0) = p_\perp. \quad (2.10)$$

This electron group is present within the pinch layer $|x| \leq x_0$, where x_0 is the positive root of the equation

$$e|A(x_0)|/c = 2p_F. \quad (2.11)$$

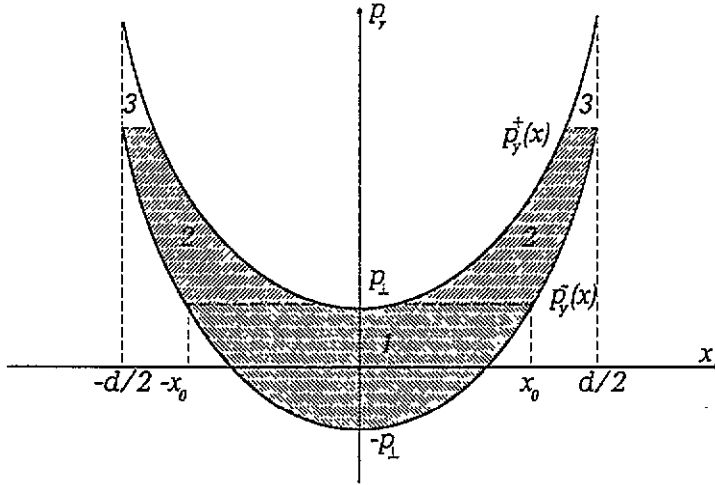


Figure 2. Phase space (p_y, x) and regions occupied by the groups of the trapped (1), Larmor (2) and surface (3) electrons.

2.2.2. *Larmor electrons.* These electrons are characterized by trajectories of type 2 in figure 1. The half period of their motion is defined by (2.8). However, the turn points $x_1 < x_2$ are roots of the equations

$$p_y^-(x) = p_y \quad p_y^+(x) = p_y. \tag{2.12}$$

The range of momentum space (p_\perp, p_y) appropriate to this electron group is

$$0 \leq p_\perp \leq p_F \quad p_y^-(x) \leq p_y \leq p_y^+(x). \tag{2.13}$$

2.2.3. *Surface electrons.* The trajectories of these electrons are presented in figure 1 by curves 3. The momentum space range occupied by them is

$$e(A(x) - A(d/2))/2c \leq p_\perp \leq p_F \quad p_y^-(d/2) \leq p_y \leq p_y^+(x). \tag{2.14}$$

In the case of diffuse electron scattering, the contribution of the surface electrons to the current is found to be small: its relative value is of the order of $R/l \ll 1$. Therefore, we shall not include them in the following calculation of the current density.

2.3. Current density of the trapped and Larmor electrons

The current densities for the corresponding groups of particles are rather simple to calculate by means of standard methods for solving the kinetic equation. This equation is linearized with respect to the electric field E , while the entire non-linearity is stipulated by the magnetic field $H(x)$ in the Lorentz force. Leaving aside the calculations, we present the expression for the current density of the trapped and Larmor electrons [7]

$$j_{\text{trap,L}}(x) = \frac{3}{2\pi} \frac{\sigma_0 E}{p_F^2 l} \int_{O_{\text{trap,L}}} \frac{dp_\perp dp_y p_\perp v_y(x)}{(p_F^2 - p_\perp^2)^{1/2} |v_x(x)|} \left(\int_{x_1}^x \frac{dx' v_y(x')}{|v_x(x')|} \text{sh}(\nu\tau(x; x')) \right. \\ \left. + \frac{\text{ch}(\nu\tau(x_1; x))}{\text{sh}(\nu T)} \int_{x_1}^{x_2} \frac{dx' v_y(x')}{|v_x(x')|} \text{ch}(\nu\tau(x_2; x')) \right). \tag{2.15}$$

Here $\nu = \nu_F/l$ is the frequency of the electron bulk collisions, O_{trap} and O_L are the ranges in momentum space (p_\perp, p_y) occupied by the trapped (2.10) and Larmor (2.13) electrons respectively. The quantity

$$\tau(x; x') = \int_x^{x'} \frac{dx''}{|v_x(x'')|} \quad (2.16)$$

represents the time interval of electron motion between the points x and x' .

3. Current density under conditions of the pinch effect

3.1. Asymptotic expansion of the current density

The asymptotic expansion of the current density of the trapped electrons, in powers of $\nu\tau \sim R/l \ll 1$, begins with a term that depends neither on the value $\nu\tau$ nor on the degree of inhomogeneity of the intrinsic magnetic field of the current. The value of the integral (2.15) is determined by the electrons at arbitrary incident angles onto the plane $x = 0$. Therefore, the conductivity of the trapped particles contains no small parameter, and is of the order of σ_0 [7]:

$$j_{\text{trap}}(x) \approx \sigma_0 E \quad |x| \leq x_0. \quad (3.1)$$

The main term in the expansion of the current density of the Larmor electrons is

$$j_L(x) = \frac{3}{2\pi} \frac{\sigma_0 E}{p_F^3} \int_{O_L} \frac{dp_\perp dp_y p_\perp v_y(x)}{|v_z| |v_x(x)| T} \int_{x_1}^{x_2} \frac{dx' v_y(x')}{|v_x(x')|}. \quad (3.2)$$

Integrating by parts over x' in (3.2), and changing the order of integration, we obtain

$$j_L(x) = -\frac{3}{2\pi} \frac{\sigma_0 E m c}{p_F^3 e} \int_{x_{1\min}(x)}^{x_{2\max}(x)} \frac{dx' d\dot{H}(x')/dx'}{H^2(x')} \int_{O_L^+(x, x')} \frac{dp_\perp dp_y p_\perp v_y(x) |v_x(x')|}{|v_z| |v_x(x)| T}. \quad (3.3)$$

The turn points $x_{1\min}$ and $x_{2\max}$ are roots of the equations

$$p_y^+(x_{1\min}) = p_y^-(x) \quad p_y^-(x_{2\max}) = p_y^+(x). \quad (3.4)$$

The range $O_L^+(x, x')$ of the momentum space is defined by the following inequalities:

$$e[A(x) - A(x')]/2c \leq p_\perp \leq p_F \quad p_y^-(x') \leq p_y \leq p_y^+(x) \quad x \leq x' \quad (3.5)$$

$$e[A(x') - A(x)]/2c \leq p_\perp \leq p_F \quad p_y^-(x) \leq p_y \leq p_y^+(x') \quad x' \leq x. \quad (3.6)$$

The expansion term (3.3) of the current density of the Larmor particles is non-zero because of the inhomogeneity of the magnetic field. This means that the conductivity of the Larmor electrons in the ground approach with respect to the parameter $\nu\tau \sim R/l \ll 1$ is connected with the drift of their orbits in the field $H(x)$. Note that the relationship between the quantities $j_L(x)$ and $dH(x)/dx$ is non-local. The next term of this expansion gives the known expression for the magnetoconductivity

$$\sigma_M = \sigma_0 \frac{R^2(x)}{l^2} \quad R(x) = \frac{c p_F}{e |\dot{H}(x)|}. \quad (3.7)$$

We shall neglect this current, since it is small in comparison with (3.3).

3.2. Trajectory current transfer and sign-alternating current structure

The Larmor electrons move in a strong magnetic field of constant sign. Therefore, one would expect that the conductivity of this electron group will be less than the conductivity of the trapped electrons. Taking this into account, we shall solve the problem of the current density distribution over the thickness of the plate by an iterative method.

In the ground approximation we consider only the contribution of the trapped electrons to the current. The corresponding current distribution, describing the pinch effect [7], has the following form:

$$j^{(0)}(x) = j_{\text{trap}}(x) = \begin{cases} \sigma_0 E & |x| \leq x_0 \\ 0 & x_0 \leq |x| \leq d/2. \end{cases} \tag{3.8}$$

The current-voltage characteristics of the plate in this approximation has a parabolic shape: $V \propto I^2$. The distribution of the intrinsic magnetic field of the current (3.8) is

$$H^{(0)}(x) = \begin{cases} -H(x/x_0) & |x| \leq x_0 \\ -H \text{sign}(x) & x_0 \leq |x| \leq d/2 \end{cases} \tag{3.9}$$

with

$$x_0 = 4R.$$

Taking into account that the function $j(x)$ is even, we shall carry out further analysis of the current structure assuming

$$0 \leq x \leq d/2. \tag{3.10}$$

In the next approximation we have to consider the contribution of the Larmor electrons to the current. For this purpose, using the magnetostatic equation (2.1) and the asymptotic expression (3.3), one can obtain the integral equation for the current density of the Larmor electrons:

$$j_L(x) = -\frac{\alpha}{2R} \int_{x_{1\min}}^{x_{2\max}} dx' j_{\text{trap}}(x') K\left(\frac{x}{2R}, \frac{x'}{2R}\right) - \frac{\alpha}{2R} \int_{x_{1\min}}^{x_{2\max}} dx' j_L(x') K\left(\frac{x}{2R}, \frac{x'}{2R}\right). \tag{3.11}$$

The expression for the kernel K is very complex and cumbersome because of the inhomogeneity of the intrinsic magnetic field of the current. If this inhomogeneity is neglected, the kernel K becomes

$$K\left(\frac{x}{2R}, \frac{x'}{2R}\right) = K\left(\frac{x-x'}{2R}\right) \tag{3.12}$$

where

$$K(t) = \frac{\pi}{8} t \left((2-t^2) \ln \frac{1+(1-t^2)^{1/2}}{1-(1-t^2)^{1/2}} - 2(1-t^2)^{1/2} \right) \quad |t| \leq 1. \tag{3.13}$$

The integration limits in (3.11) in this case are

$$x_{1\min} = \max\{0, x - 2R\} \quad x_{2\max} = \min\{d/2, x + 2R\}. \tag{3.14}$$

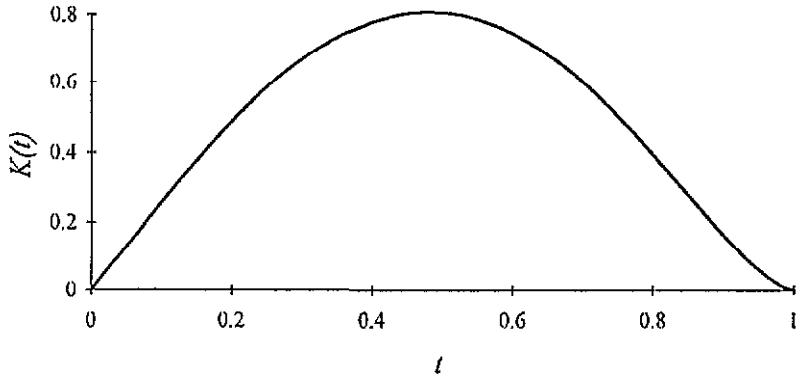


Figure 3. Plot of the kernel $K(t)$ (see (3.13)).

Note that $K(t)$ is an odd function, being positive at $t > 0$. Its plot at $t > 0$ is given in figure 3.

The parameter α is

$$\alpha = \frac{6}{\pi^2} \frac{\sigma_0 ER}{I} < 1. \quad (3.15)$$

By means of (3.8) and (3.9) one can easily ensure that this value does not depend on any parameter of the problem, and is a number less than unity. According to (3.11), the parameter α represents the coefficient of the current transfer from the pinch layer $|x| < x_0$ to the periphery and between the neighbouring Larmor current layers. Therefore, we can present the solution of (3.11) as a series:

$$j_L(x) = \sum_{n=1}^{\infty} j_L^{(n)}(x) \quad (3.16)$$

where

$$j_L^{(1)}(x) = -\frac{\alpha}{2R} \int_{x_{1\min}}^{x_{2\max}} dx' j_{\text{trap}}(x') K\left(\frac{x-x'}{2R}\right) \quad (3.17)$$

$$j_L^{(n)}(x) = -\frac{\alpha}{2R} \int_{x_{1\min}}^{x_{2\max}} dx' j_L^{(n-1)}(x') K\left(\frac{x-x'}{2R}\right) \quad n = 2, 3, \dots \quad (3.18)$$

Note that the absolute value of each subsequent term in the series (3.16) is $\alpha^{-1} > 1$ times smaller than the previous one.

Let us consider the first term in this series. As follows from (3.8), (3.14) and (3.17), the current density $j_L^{(1)}$ differs from zero in the spatial layer

$$0 \leq x \leq x_0 + 2R. \quad (3.19)$$

This term determines a small correction to j_{trap} in the interval $0 \leq x \leq x_0$ and is essential in a layer

$$x_0 \leq x \leq x_0 + 2R. \quad (3.20)$$

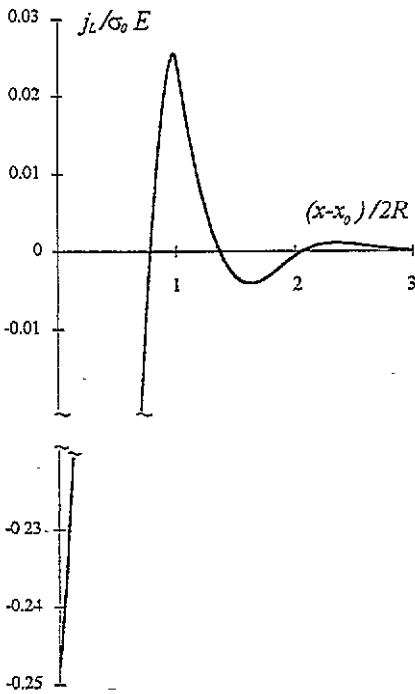


Figure 4. Spatial distribution of the current of the Larmor electrons calculated for $\alpha = 0.3$.

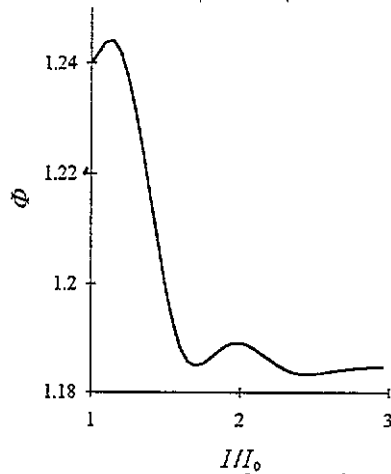


Figure 5. Dependence of the oscillating factor Φ on the dimensionless current I/I_0 for $\alpha = 0.5$.

The current density $j_L^{(1)}$ is a sign-alternating function of x . It proves to be negative in the layer (3.20). The appearance of a current flowing in a direction opposite to the electric field E is caused by a current transfer from the pinch layer.

The second term in the series (3.16) is non-zero in the interval $0 \leq x \leq x_0 + 4R$. It gives an addition to the currents j_{top} and $j_L^{(1)}$ in the region (3.19) and determines the main contribution to the current within a layer

$$x_0 + 2R \leq x \leq x_0 + 4R. \tag{3.21}$$

The current density $j_L^{(2)}$ proves to be positive here. The excitation of the current in the layer (3.21) is a result of the current transfer from the region (3.20).

Continuing this analysis, we find that the term $j_L^{(n)}$ is non-zero in the interval $0 \leq x \leq x_0 + 2Rn$, but its contribution to the current (3.16) is the main contribution in the region

$$x_0 + 2R(n - 1) \leq x \leq x_0 + 2Rn. \tag{3.22}$$

The current $j_L^{(n)}$ in the layer (3.22) will be positive if n is even, and negative if n is odd.

Therefore, the sign-alternating current structure arises in the plate owing to the trajectory transfer of the current by the Larmor electrons. The peripheral part of the sample is found to be broken into Larmor-current layers with a thickness of about $2R$. The current density alternates in sign and decreases in magnitude from one layer to another. Figure 4 shows the current structure calculated numerically on the basis of (3.16) for $\alpha = 0.3$. We note the fact that the thicknesses of the Larmor-current layers do not equal $2R$ for finite α . In this case several neighbouring terms in the sum (3.16) give a contribution to the current density within each layer. The thickness of each Larmor-current layer tends to $2R$ with $\alpha \rightarrow 0$.

It is clear that only a finite number of Larmor-current layers can be contained inside the periphery part $x_0 < x < d/2$ of the plate. This number depends on the current I and the plate thickness d . This dependence provides the CVC oscillations.

4. Current-voltage characteristics

We now turn to a derivation of the CVC of the plate under pinch-effect conditions. For this purpose it is necessary to calculate the total current transported by the trapped and Larmor particles:

$$I = I_{\text{trap}} + I_L. \quad (4.1)$$

To obtain the current of the trapped electrons we can use (3.1) for $j_{\text{trap}}(x)$, which leads to

$$I_{\text{trap}} = 8R\sigma_0 E. \quad (4.2)$$

The current of the Larmor particles can be calculated by the formula

$$I_L = 2 \int_0^{d/2} dx j_L(x). \quad (4.3)$$

Substituting (3.11) for the Larmor current density $j_L(x)$ into (4.3) and changing the order of integration over x and x' , we obtain the following expression:

$$I_L = -2\alpha \int_0^{2R} dx (\sigma_0 E + j_L(x)) F\left(\frac{x}{2R}\right) + 2\alpha \int_{-2R+d/2}^{d/2} dx j_L(x) F\left(\frac{-x+d/2}{2R}\right) \quad (4.4)$$

$$F(t) = \int_t^1 dt' K(t'). \quad (4.5)$$

We pay particular attention to the second integral in (4.4). It can be seen that the interval of integration includes the surface Larmor-current layer. As follows from the analysis carried out in section 3, the current density alternates in sign with increasing I in a quasiperiodical manner because the total number of Larmor-current layers depends on I . Thus the second term in (4.4) represents an oscillating function of the total current. As for the first term in (4.4), it changes monotonically with I .

After substituting (4.2) and (4.4) into (4.1), and making some simple transformations, we arrive at the following result for the CVC of the plate:

$$\frac{V}{V_0} = \left(\frac{I}{I_0}\right)^2 \Phi\left(\frac{I}{I_0}\right) \quad V_0 = \frac{4c^2 p_F L}{\pi e \sigma_0 d^2} \quad I_0 = \frac{4c^2 p_F}{\pi e d} \quad (4.6)$$

$$\Phi\left(\frac{I}{I_0}\right) = \left[1 - \frac{\alpha}{4R} \int_0^{2R} dx \left(1 + \frac{j_L(x)}{\sigma_0 E} - \frac{j_L(-x+d/2)}{\sigma_0 E}\right) F\left(\frac{x}{2R}\right)\right]^{-1}. \quad (4.7)$$

Here V_0 and I_0 represent the characteristic values of the voltage and current, respectively, at which the thickness $2x_0$ of the pinch layer is about the sample thickness d , L is the sample

size along the direction of current flow (along the y axis). Note that (4.6) is valid when condition (1.7) for the pinch effect is fulfilled. i.e. at

$$I > I_0. \quad (4.8)$$

Expression (4.6) contains two multipliers. The first of them, changing quadratically with current, is caused by the contribution of the trapped particles. Taking account of the Larmor electrons results in the appearance of the second multiplier, Φ , which oscillates with increasing I . The period of such anharmonic oscillations is about I_0 ; the magnitude of the oscillations decreases (as the current I increases) in an exponential manner, proportional to α^{I/I_0} . The dependence of the oscillating factor Φ on I/I_0 in the range (4.8) of strong currents is presented in figure 5. This plot was calculated on the basis of (4.6), (4.7) and (3.16) for $\alpha = 0.5$.

5. Experiment and discussion

We measured the electrical resistances of the rectangular tungsten plates by a four-contact method. The plates were cut from crystal bars on an electrical arc machine. The ratio $\rho_{300}/\rho_{4.2}$ of the resistances at 300 and 4.2 K was equal to 80 000. The plates were mechanically polished and then etched in a mixture of concentrated nitric, fluoric and orthophosphoric acids. In order to fabricate reliable current contacts, we electroplated a 10 μm -thick layer of tin on the ends of the plates and then soldered copper wires to the tin. The voltage leads (0.06 mm diameter platinum wire) were welded to the plates by discharging a capacitor. The current and voltage contacts were separated by a distance of 2–3 mm, and the voltage contacts were spaced at least 4 mm apart.

The dimensions of the plates were $9 \times 0.4 \times 0.14 \text{ mm}^3$ (W1), $9 \times 0.27 \times 0.09 \text{ mm}^3$ (W2), $13 \times 2 \times 0.03 \text{ mm}^3$ (W3), $12 \times 0.7 \times 0.12 \text{ mm}^3$ (W4). All plates had the same orientation, with the large face along the (100) plane.

In the experiment we recorded the CVC of the plates and the current dependence of the resistance. The I - V characteristics were recorded by a Hewlett-Packard model 3390 integrating potentiometer. A DC current potentiometer measured the resistance. Considerably more accurate results were obtained by a modulation technique, which enabled us to measure the differential resistance \mathcal{R} and record continuous traces $\mathcal{R}(I)$ by harmonically modulating the current at low frequency and using a selective amplifier and phase detector to select the signal (proportional to dV/dI) at the modulation frequency. This frequency was low enough so that the skin effect was negligible. Most of the measurements were made at 10 Hz. The amplitude of the modulation current was 0.2–0.3 A.

The ratio $\rho_{300}/\rho_{4.2}$ was 4000–10 000 for our plates, which was much less than that in the starting bars. Resistance measurements in an external longitudinal magnetic field H_y revealed that the thinness of the plates, rather than the deformation of the plates, was primarily responsible for these small values. Applying the field H_y increased $\rho_{300}/\rho_{4.2}$ almost to the value for the initial bar. Thus for sample W1 ($\rho_{300}/\rho_{4.2} = 8000$), the application of the longitudinal field decreased the resistance by almost tenfold. We estimated the mean free path l from the known values of ρl and found that $l = 3 \text{ mm}$ at $T = 1.5 \text{ K}$.

Since $\mathcal{R}(I)$ was measured for $I < 50 \text{ A}$, less than 0.1 W cm^{-2} of power was evolved in the samples.

Figure 6 shows a plot of the dependence of the differential resistance \mathcal{R} on the current I obtained for the sample W2 at a temperature $T = 1.5 \text{ K}$. A similar behavior for $\mathcal{R}(I)$

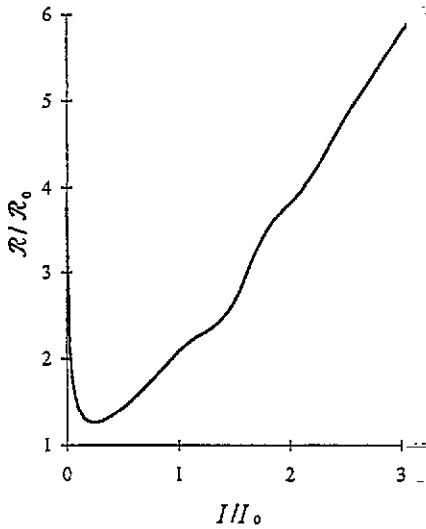


Figure 6. Record of the dependence of the differential resistance on the current obtained for the sample W2 at $T = 1.5$ K.

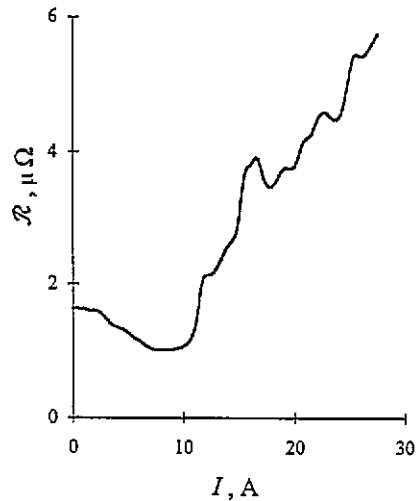


Figure 7. Dependence of the differential resistance on the current at $l/d = 30$ and $\alpha = 0.5$, $R_0 = V_0/I_0$.

was observed for all samples investigated within the whole temperature interval where (1.1) is fulfilled. In accordance with the theoretical predictions of [1, 2], the reduction in the resistance takes place in the range of weak currents. As was mentioned in the introduction, this phenomenon is caused by the appearance of the trapped electron group in the sample under conditions (1.5). At a value of $I \approx 8$ A the decrease in the resistance is superseded with a nearly linear increase. Decaying oscillations of $\mathcal{R}(I)$ are well defined on the background of this linear portion.

In order to compare experimental results with theoretical conclusions we have constructed in figure 7 the interpolational curve $\mathcal{R}(I)$, which combines the results of [1, 2] (for the drop portion) and of this paper. A convenient interpolational formula for the CVC was proposed in [7]. However, this formula does not take into account the conductivity of the Larmor electrons and does not describe the CVC oscillations. Therefore, we used it only for a description of the $\mathcal{R}(I)$ portion in the range $I/I_0 < 1$. The ratio $l/d = 30$ characterizes the sample W2 at $T = 1.5$ K, and just this value was chosen for calculations. The $\mathcal{R}(I)$ plot in the range of strong currents $I/I_0 > 1$ (the oscillating portion) is constructed on the basis of (4.6) at $\alpha = 0.5$. Both formulae used give the same value for \mathcal{R} at the point $I/I_0 = 1$.

A comparison of figures 6 and 7 shows their qualitative agreement. Since the sign-alternating current structure is a natural feature of the pinch effect in metals, we can conclude that this stipulates the experimentally observed $\mathcal{R}(I)$ oscillations. Unfortunately, for several reasons, we cannot carry out a quantitative comparison of the curves in figures 6 and 7. First, our theory is constructed for the case of strong currents in the range (4.8) where the inequality (1.7) holds. Therefore, the theory can quantitatively describe oscillations with high numbers, but is applicable only qualitatively for the real experiment where several early oscillations at $R \sim d$ are observed. Furthermore, a plate always has a finite width, a fact that was not taken into account in the theory. At the same time, the widths of all experimental samples were less than the electron free path. For this reason the spatial distribution of the intrinsic magnetic field of the current possessed more complex structure, which affected the

current transfer from the pinch layer to the periphery. To analyse this factor one should consider theoretically the sign-alternating current structure in an experimentally realizable geometry, namely in a wire.

As well as oscillations of the CVC, auto-oscillations of the voltage in the regime of the designated current were observed in [6] in the range of strong currents. We believe that the nature of the auto-generation is related to the sign-alternating current structure analysed here. Indeed, the layers, where the current flows in the opposite direction to the electric field, arise in the sample as a result of current transfer. This unusual current distribution may be the reason for the instability of the stationary state. The problem of the instability of the described current structure is of principal interest.

In conclusion, we note that a sign-alternating current structure, similar to the one studied in this work, also arises under conditions of the static skin-effect [8]. In this case the trajectories of the Larmor electrons are formed by a strong external uniform magnetic field and a rather weak non-uniform intrinsic magnetic field of a current. The sign-alternating current distribution occurs as a result of the current transfer from the static skin-layers into the sample bulk. The number of Larmor-current layers depends on the values of the external magnetic field and the sample thickness. On the basis of the analysis carried out in this work, we can conclude that an oscillating dependence of the voltage on the value of the external magnetic field should be observed under conditions of the static skin-effect.

Acknowledgments

This work was made possible in part by grant No N3F000 from the International Science Foundation and was supported in part by the Ukrainian Committee on Science and Technology (project No 2.3/19 'Metal'), the Russian Fundamental Science Foundation (project No 93-02-2039), and the Ukrainian grant for young scientists (project 'Oscillation').

References

- [1] Kaner E A, Makarov N M, Snapiro I B and Yampol'skii V A 1984 *Pis'ma Zh. Exp. Teor. Fiz.* **39** 384 (Engl. transl. 1984 *JETP Lett.* **39** 463)
- [2] Kaner E A, Makarov N M, Snapiro I B and Yampol'skii V A 1984 *Zh. Exp. Teor. Fiz.* **87** 2166 (Engl. transl. 1984 *Sov. Phys.-JETP* **60** 1252)
- [3] Aleksandrov B N 1962 *Zh. Exp. Teor. Fiz.* **43** 1231 (Engl. transl. 1963 *Sov. Phys.-JETP* **16** 871)
- [4] Yaqub M and Cochran J F 1963 *Phys. Rev. Lett.* **10** 390
- [5] Voloshin I F, Kravchenko S V, Podlevskikh N A and Fisher L M 1985 *Zh. Exp. Teor. Fiz.* **89** 233 (Engl. transl. 1985 *Sov. Phys.-JETP* **62** 132)
- [6] Zakharchenko S I, Kravchenko S V and Fisher L M 1986 *Zh. Exp. Teor. Fiz.* **91** 660 (Engl. transl. 1986 *Sov. Phys.-JETP* **64** 390)
- [7] Kaner E A, Leonov Yu G, Makarov N M and Yampol'skii V A 1987 *Zh. Exp. Teor. Fiz.* **93** 2020 (Engl. transl. 1987 *Sov. Phys.-JETP* **66** 1153)
- [8] Leonov Yu G, Makarov N M and Yampol'skii V A 1989 *Zh. Exp. Teor. Fiz.* **96** 1764 (Engl. transl. 1989 *Sov. Phys.-JETP* **69** 996)